Biologically-Inspired Locomotion of a 2g Hexapod Robot

Andrew T. Baisch, *Student Member, IEEE*, Pratheev S. Sreetharan, and Robert J. Wood, *Member, IEEE*

***Abstract*— Here we present the design, modeling, and fabrication of a 2g mobile robot. By applying principles from biology and existing meso-scale fabrication techniques, a 5.7cm hexapod robot with sprawled posture has been created, and is capable of locomotion up to 4 body-lengths per second using the alternating tripod gait at 20Hz actuation frequency. Furthermore, this work proves the viability of a new mechanical linkage design, fabricated using the smart composite microstructure process, to provide desirable leg trajectories for successful ambulation at the insect-scale.**

I. Introduction

Autonomous mobile robots are a desirable alternative to sending humans into hazardous environments such as areas affected by natural disaster. Small and agile robots would be invaluable in scenarios such as exploration of a collapsed building, where they could provide reconnaissance to rescue workers including survivor locations and chemical toxicity levels. Furthermore, in these missions, large numbers of agile robots using swarm algorithms would be preferred over larger robots for their efficiency and cost.

While developing small walking robots, it is useful to study animal locomotion at the same scale, where we find a number of nature's most agile runners. One example, the cockroach (order *Blattaria*), is capable of high-speed locomotion up to 40 body-lengths per second [1], stable rapid running over rough terrain [2], and can scale vertical or inverted surfaces [3]. Two fundamental hexapod characteristics contributing to the cockroach's locomotion prowess are a sprawled posture [4] and alternating tripod gait [1], [5], [6], which therefore have applications in ambulatory microrobots. Proof of this lies in the numerous successful applications of these principles in hexapod robots that achieve robust locomotion over a variety of terrains: RoACH [7], DASH [8], RHex [9], Mini-Whegs [10], iSprawl [11], and Sprawlita [12].

Multiple challenging locomotion modes (i.e. climbing vertical and inverted surfaces), are favorable at smaller scales; as characteristic length decreases, surface (adhesion) forces begin to dominate volumetric (inertial) forces [13]. Previous work proved the feasibility of fabricating a crawling insect-scale robot capable of forward locomotion on flat ground [14], and the results motivated multiple improvements in design, fabrication, and actuation which are presented here. By applying the above principles from biology and utilizing the smart composite microstructure (SCM) fabrication process, the second Harvard Ambulatory MicroRobot ($HAMR^2$) was created. The results are a 5.7cm long and 2g robot, capable of tethered locomotion up to 4 body-lengths per second.

Here, the detailed robot design will be presented, highlighting the conceptualization and analysis of a new flexure-based linkage, actuator selection, and mechanical/electrical integration. The meso-scale fabrication techniques used to instantiate an insect-scale walking robot are also discussed. Finally, the resulting locomotion capabilities are presented, along with current and future work towards a highly-agile, autonomous, insect-scale hexapod robot.

The authors are with the School of Engineering and Applied Sciences, Harvard University, Cambridge, MA 02138, USA (contact e-mail: abaisch@seas.harvard.edu)

II. Robot Design

The goal of this work was to address necessary improvements in locomotion performance and fabrication difficulty of a centimeter-scale robot capable of flat ground locomotion. Design choices were made considering their implications to future work as well, including scalability and enablement of more challenging locomotion modes (e.g. rough terrain and climbing). Consistent with cockroaches, the robot was designed with a sprawled posture to favor dynamic stability and climbing ability by maintaining center-of-mass (COM) close to the walking surface [15]. Similar to the central pattern generator in cockroaches, the robot walks open-loop using the alternating tripod gait.

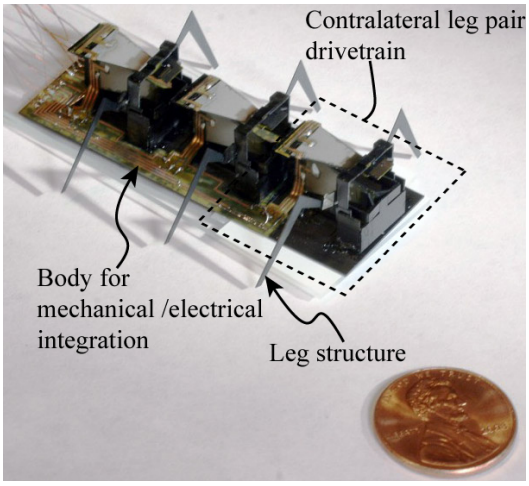

Fig. 1. The second generation Harvard Ambulatory MicroRobot.

When considering the heavy cost (i.e. increased size, power consumption, and fabrication complexity) that is incurred per additional actuator, a minimalist approach to the mechanical design of a hexapod microrobot is preferable. $HAMR^2$ therefore has six total actuators, grouped in pairs on three identical segments. Each segment is comprised of

all components necessary to drive two contralateral legs, and are modular to decrease fabrication difficulty, as will be discussed in Section III. The mechanics and electronics of the three segments are integrated by a single body, detailed in Section II-C.

A. Mechanical Design

A minimum of two degrees of freedom per leg, 'lift' and 'swing', are required to achieve the desired alternating tripod gait. The lift degree of freedom, labeled θ, provides motion orthogonal to the walking plane, serving to raise legs belonging to the inactive tripod off of the walking surface. The swing degree of freedom, ϕ provides motion in the walking plane and is the primary vector by which locomotive power is applied. Furthermore, the ideal leg mechanism minimizes actuation complexity while concentrating mass proximal to the body. To achieve these design goals using flexure joints consistent with the SCM fabrication process (Section III), a new spherical five-bar (SFB) linkage was created.

The SFB maps two decoupled drive inputs to a 2DOF output leg motion (See Fig. 2). The SFB is a parallel mechanism with both input links executing simple rotations with respect to the linkage ground. Since all actuation is simply referenced to the robotic body, actuation mass can be proximally concentrated. This mass distribution enabled by the parallel SFB is a distinct improvement over previous designs which required actuation of distal links of a serial kinematic chain [14].

From the neutral configuration, actuation of the swing input causes a rotation of the output leg about an axis perpendicular to the walking plane through the SFB spherical center. The foot executes an arc in the walking plane, a departure from ideal linear motion, due to the inherent SFB kinematics and undesirable compliance within the flexure-based transmission. Independent of leg swing angle, actuation of the lift input causes an output leg rotation about an axis in the walking plane perpendicular to the leg and through the SFB spherical center.

The two inputs to the SFB are largely decoupled, providing independent control of lift and swing angles. Fig. 3 compares the ideal decoupled leg trajectory with that realized by the SFB. The decoupled leg motion results in a simple mapping between actuation inputs and leg orientation, simplifying control system design.

Furthermore, inputs to multiple SFB's referenced to the body can be mechanically coupled by simple planar linkages to greatly reduce actuation complexity. In HAMR^2, a SFB drives each of the six legs, providing twelve nominal actuation inputs. However, the alternating tripod gait may be achieved with a minimum two linear actuators as in RoACH [7]. Here, a modular design is used to reduce fabrication complexity (see Section II-C), and therefore pairs of lift and swing inputs are coupled across the body: lifting one leg lowers the contralateral leg, while an anterior swing of one leg is coupled to a posterior swing of the contralateral leg. The contralateral coupling reduces the twelve degrees of freedom to six, allowing an alternating tripod gait to be achieved with six actuators.

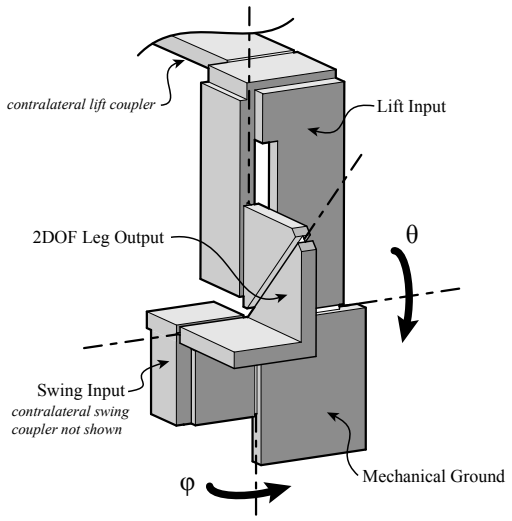

Fig. 2. The spherical five-bar (SFB) linkage used to drive two leg DOFs, θ (lift) and ϕ (swing).

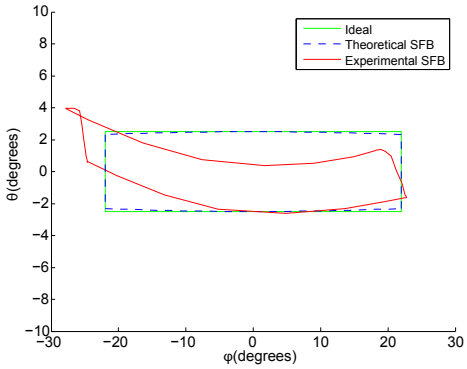

Fig. 3. SFB linkage coupling curve. Theoretically, the SFB follows close to an ideal (rectangular, decoupled) trajectory. The example experimental trajectory is repeatable for a single leg, however deviates from nominal due to fabrication error and undesired compliances.

B. Actuation

To drive the SFB transmissions, HAMR^2 uses six piezoelectric actuators, chosen over alternatives such as shape memory alloy and DC motors since they are favorable in several measurable categories: bandwidth, power density, and force output. One could argue that DC motors have similar, if not better characteristics in these regards, however qualities such as scalability and ease of integration into the preferred fabrication technique further motivate the selection of piezoelectrics. Taking advantage of existing modeling, design, and fabrication techniques for a piezoelectric actuator, an optimal energy density cantilever geometry [16] was chosen to minimize actuator mass for given force and displacement requirements, thereby reducing the energy necessary for locomotion. Furthermore, the bimorph actuator, with PZT-5H

piezoelectric layers (Piezo Systems Inc. www.piezo.com) and a single carbon fiber elastic layer, has been proven suitable for microrobot applications [17], [18], and is easily integrated into the fabrication process described in Section III.

Two actuators for a contralaterally-coupled SFB pair are mounted orthogonally using the structure shown in Fig. 4a. The structure provides a rigid mechanical ground while locating actuators low and proximal to the body, favoring stability and efficiency. Actuator outputs are mapped to the SFB using planar linkages shown in Fig. 4b (along with an unfolded actuator mount). The full lift and swing drivetrain kinematics, including planar input linkages and decoupled SFB DOFs, are detailed in Fig. 5.

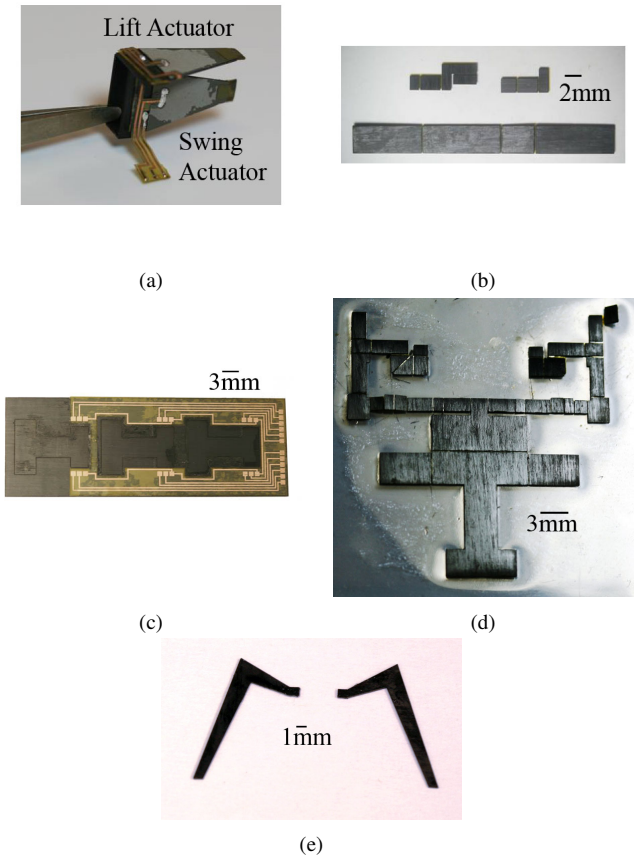

Fig. 4. Components of the second generation Harvard Ambulatory MicroRobot: (a) Lift and swing actuators, mounted orthogonally. (b) Planar input transmissions that map actuator output to the SFB lift (top left) and swing (top right) DOFs and unfolded transmission mount (bottom). (c) HAMR^2's body integrates three actuator/transmission segments both mechanically, with jigsaw cutouts, and electrically, with flex circuit bus. (d) A contralaterally-coupled spherical five-bar linkage pair, unfolded. (e) HAMR^2's legs, made from six-layer carbon fiber laminate.

C. Integration and Electronics

HAMR^2's three identical segments are integrated by a single body, which provides both a mechanical ground and electrical bus to trace actuator signals from off-board power and control (See Fig. 4c). The body, fabricated using techniques consistent with the SCM process in Section III,

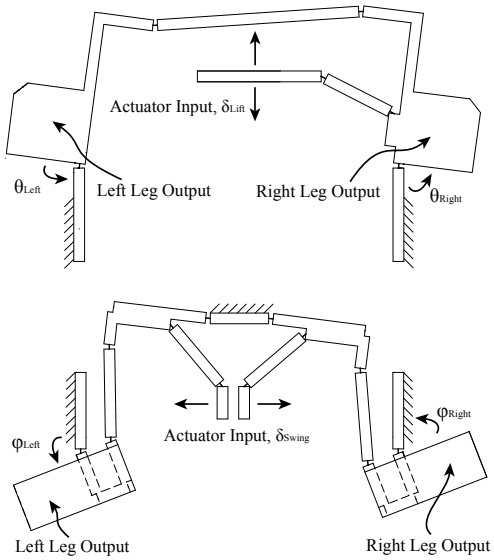

Fig. 5. Decoupled drivetrain planar kinematics. The lift (top) is used to raise legs from the walking surface while the swing (bottom) provides power for locomotion in the walking plane.

is six laminated fiber composite layers, each having fiber orientation orthogonal to the subsequent layer, providing a rigid mechanical ground. The top three layers are patterned with slots, such that each of the three segments fits perfectly into the body, and no manual alignment is necessary. This feature of modularity also decreases the tedium normally associated with fabrication, since a single failure only affects one third of the robot, and damaged sections may be removed for debugging.

A flex circuit bus bonded to the body traces externally-generated drive signals from wires, attached at the robot's anterior, to the piezoelectric actuators. This integrated circuitry, the fabrication of which is described in Section III, is a vast improvement from previous work, where wires protruding from multiple directions obstructed locomotion. Furthermore, the onboard bus should be capable of housing embedded components such as piezoelectric drive circuitry [19] in future work.

D. Parameter Selection

Robot parameters were selected by integrating models of hexapod locomotion, SFB kinematics, and piezoelectric bimorph actuators. Numerous mathematical models exist in literature [20] that form a basis for selecting appropriate inputs and body morphology parameters for insect-scale hexapod locomotion. However, the simplest of these models [21], which deals exclusively with the horizontal (walking) plane, requires a total of two actuators per leg, even when neglecting the lift DOF. While this model accurately predicts cockroach behavior it would be a gross overuse of actuators for a microrobot. Therefore, a similar, but simpler model was constructed such that each leg is actuated by a single torque at its hip joint. The model was used to obtain a conservative

estimate of the necessary hip-torque inputs to achieve the desired locomotion of a hexapod robot.

Decoupled horizontal and vertical plane kinematic models of the SFB (See Fig. 5) were created, assuming swing and lift DOFs are sufficiently decoupled. The swing plane model quasi-statically maps hip torque approximations from horizontal-plane dynamics to the actuator output, ensuring actuator force and displacement outputs sufficient for locomotion. Similarly, lift plane kinematics ensure that actuator outputs are sufficient to lift the robot. An existing actuator model [16] was used to determine geometric parameters for an energy density-optimizing piezoelectric cantilever, using conservative estimates of necessary actuator outputs obtained from the dynamic and kinematic models. The results of this analysis yielded HAMR^2's design parameters, summarized in Table I.

III. Fabrication

HAMR^2's SCM parts were fabricated using the process detailed in [22], with improvements to increase mechanism robustness. The spherical joint, composed of five planar flexures, requires all joint axes to intersect at a point to be nonsingular. Therefore, each SFB must be generated as a single SCM part to eliminate the human error associated with manually aligning and mating multiple parts. As shown in Fig. 4d, the unfolded SFB has primary link axes in multiple directions and would benefit from orthotropic material properties. However, typical SCM parts use single-layer composites, and cut files are designed to account for a single fiber orientation. An addition to the existing fabrication process uses two-layer composites with orthogonal fiber orientations, providing the requisite rigidity to all links. The SCM fabrication process using orthotropic links is detailed in Fig. 6.

Compliant leg structures for a microrobot are an ongoing research topic, and therefore were not included in this work. Here, legs were fabricated similarly to the body, using a six-layer composite to prevent buckling under the robot's weight.

Copper-Kapton laminate flex circuits, which trace externally-generated signals to HAMR^2's actuators, were created and easily integrated using the same diode-pumped solid-state (DPSS) laser micromachining system as the SCM process. A lithography process was developed that runs the DPSS laser at low power to selectively ablate spun photoresist without damaging the underlying metal. The remaining processing steps require a copper wet etch, resist strip, and subsequent release of the flex circuits from their processing substrate. The resulting flex circuits, shown in Fig. 4c, have copper traces as small as $200\mu m$, but trace widths on the order of $10\mu m$ have been achieved. The total fabrication time for a single robot (part generation and manual assembly), is roughly one week.

IV. Results

The resulting robot, HAMR^2, has physical specifications summarized in Table I. Drive signals are generated and interfaced with a high-voltage power supply using Simulink

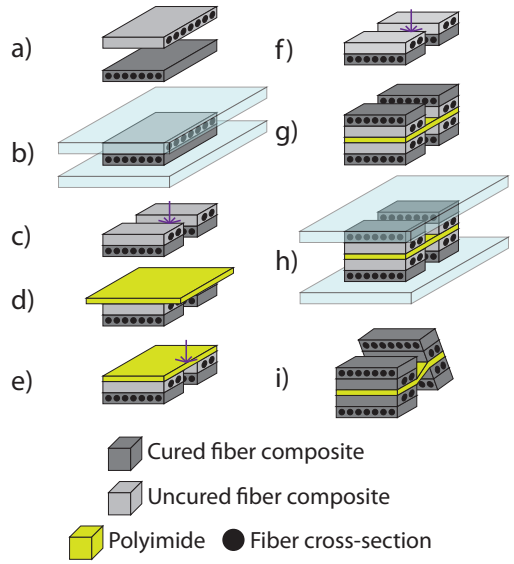

Fig. 6. The smart composite microstrucutre (SCM) fabrication process with orthotropic structural layer material properties. Single sheets of cured and uncured fiber composites (a) are pre-cured under vacuum, with fibers oriented orthogonally (b). The pre-cured sheets are patterned with a diode-pumped solid state (DPSS) laser micromachining system (c). A polyimide layer is laminated to the patterned composite (d) and cut with different laser settings (e). A second precured fiber-composite layer is laser-cut (f) and optically-aligned with the other composite and polymer layers (g). The five-layer laminated structure is then cured under vacuum (h). The resulting microstructure, with orthotropic material properties, has compliant flexure joints that may be folded and fixed to create 3D structures or left to articulate (i). Using this process, parts may be designed without regard to fiber orientation.

TABLE I

HAMR^2 DESIGN SPECS. *DENOTES EMPIRICALLY DETERMINED VALUES

Body length $57mm$	Foot-to-foot width $35mm$
Leg length $7mm$	Leg height (from SFB spherical center) $5mm$
Mass* (no power electronics) $2.0g$	Single actuator mass* $114mg$
Actuator PZT thickness $127\mu m$	Actuator elastic thickness $80\mu m$
Actuator length $9.98mm$	Actuator nominal width $5.07mm$

and xPc target system (Mathworks). $200V$ peak-to-peak ramped square wave inputs were chosen to maximize joint torques during each step while preventing potential actuator mechanical failure. In testing the alternating tripod gait, four distinct input signals were used for the six actuators: anterior / posterior swing, center swing, anterior / posterior lift, and center lift.

Using 2D motion capture software, leg trajectories were tracked in air (See Fig. 7). Furthermore, the robot was tested on flat ground up to 20Hz actuator frequency. Fig. 8 shows straight walking at 20Hz, at which a maximum speed of 4 body-lengths per second (22.8 cm/s) was achieved. Fig. 9 summarizes the results at all tested actuator frequencies. The positive slope of these results suggest that the robot's maximum speed has not been determined, and should con-

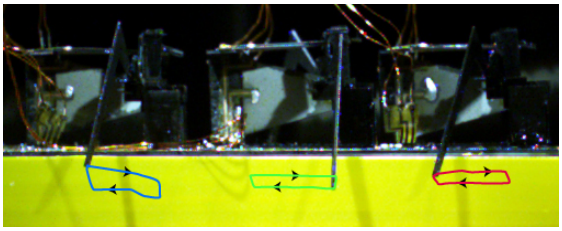

Fig. 7. Alternating tripod leg trajectories are validated by suspending HAMR^2 and tracking three ipsilateral legs. Results using ProAnalyst 2D motion tracking software show all legs nominally following the same trajectory, with center leg 180 degrees out of phase with the anterior and posterior legs.

tinue to grow with actuation frequency until a rolloff beyond mechanical resonance, or until foot-ground mechanics fail to provide a solid footing. Higher frequencies were not tested due to catastrophic failure unrelated to actuation frequency, discussed in the following section.

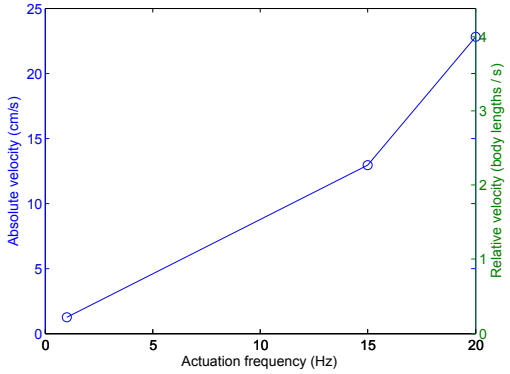

Fig. 9. Plot of HAMR^2's locomotion speed at tested actuator frequencies.

An estimated total average power was obtained by measuring individual actuator power in air. Using these values and speed measurements, a cost of transport (COT) metric (measured in energy/mass/distance) was obtained and is summarized in Fig. 10. The reported values are likely an overestimate since the power was measured in air, and more precise COT measurements are a subject of ongoing work. The resulting trend suggests that an optimal actuator frequency exists to minimize power consumption during locomotion, and will be explored in future work. Furthermore, Table II compares the estimated cost of transport to those obtained for other walking robots, as published in [8]. The comparison shows that HAMR^2's COT is significantly larger than existing walking robots, motivating attention to efficiency in future designs.

V. Conclusions and Future Work

HAMR^2 runs up to 4 body-lengths per second at actuation frequencies up to 20Hz, proving the viability of creating an insect-scale hexapod robot capable of high-speed locomotion. All chosen fabrication techniques and physical components are scalable such that future iterations could be smaller. This work also proves that the biologically-inspired

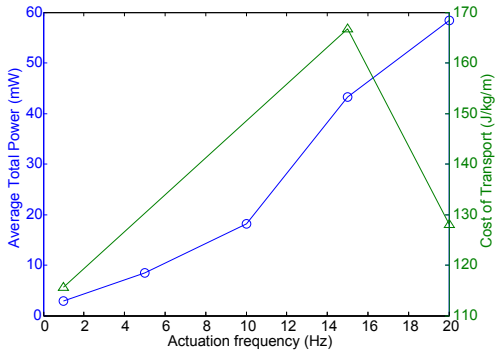

Fig. 10. Plot of power consumption (blue circles) and cost of transport (green triangles) at measured actuator frequencies.

TABLE II
Cost of transport data for various hexapod robots

Robot	Mass (g)	Cost of transport (J/kg/m)
Mini-Whegs [10]	146	8.9
DASH [8]	16.2	14.7
iSprawl [11]	300	17.4
RHex [9]	7500	20
HAMR^2	2	128

alternating tripod gait is achievable using the SFB linkage and chosen leg-coupling constraints.

Current work includes improved robustness, decreased fabrication time, intelligently-designed biomimetic leg structures, and integrated high-voltage electronics. In HAMR^2, locomotion capabilities were tested to catastrophic failure within the electronics: PZT mechanical failure induced by shorting across flex circuit traces. This issue, related to circuit trace proximity (dielectric breakdown) and environmental exposure, will be addressed in future iterations. Fabrication time exacerbates the problems of robot failure, and therefore the SCM process is constantly evolving to promote parallelization and reduce manual steps.

With a more robust device and more streamlined fabrication process, additional tests will further identify the design's locomotion capabilities. This includes turning, higher-speed locomotion, and more rigorous COT measurements. Furthermore, high-speed videography will be utilized for the characterization of walking modes (i.e. quasi-static vs. dynamic) and inform future modeling efforts.

Leg compliance and damping, which simplifies stride-level control in running [2] and climbing [15], will be a feature of future designs. Utilizing a combination of micro- and meso-scale fabrication processes, millimeter-scale robotic legs with tuned compliance will be developed. For desirable foot-ground interaction on flat and vertical surfaces, various adhesion mechanisms will be explored, including those that enable vertical locomotion such as spines [23], [15] and adhesive elastomers [24], [25]. Integration of appropriate attachment technologies into a millimeter-scale robotic leg will enable locomotion on a wide range of vertical surfaces.

Integration of piezoelectric drive circuitry into a micro-robotic fly is a topic of current work [19], and will be

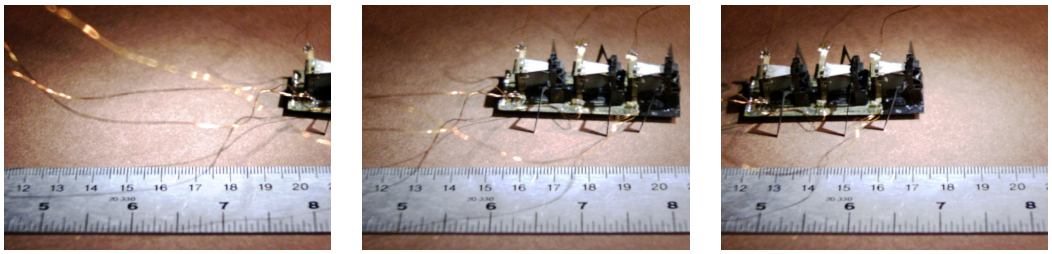

t=0s t=0.2s t=0.4s

Fig. 8. Locomotion at 20Hz actuator frequency, using the alternating tripod gait.

applied to an ambulatory robot when available. Existing fabrication techniques to embed discrete components into flex circuits will be used to provide future versions with onboard power and drive circuitry. A rough estimate of additional electronic component mass based on commercially available components totals 260mg (50mg static weight and 35mg per actuator) [26]. Onboard circuitry will provide the necessary autonomy and increased locomotion performance by eliminating external wiring.

VI. Acknowledgements

The authors gratefully acknowledge The Charles Stark Draper Laboratory and the National Science Foundation (award number IIS-0811571) for support of this work. Any opinions, findings, and conclusions or recommendations expressed in this material are those of the authors and do not necessarily reflect the views of the National Science Foundation.

References

[1] F. Delcomyn, "The locomotion of the cockroach," *J. Exp. Biol*, vol. 54, pp. 443–452, 1971.

[2] S. Sponberg and R. Full, "Neuromechanical response of musculoskeletal structures in cockroaches during rapid running on rough terrain," *Journal of Experimental Biology*, vol. 211, no. 3, p. 433, 2008.

[3] D. Goldman, T. Chen, D. Dudek, and R. Full, "Dynamics of rapid vertical climbing in cockroaches reveals a template," *Journal of Experimental Biology*, vol. 209, no. 15, p. 2990, 2006.

[4] T. Kubow and R. Full, "The role of the mechanical system in control: a hypothesis of self-stabilization in hexapedal runners," *Philosophical Transactions of the Royal Society B: Biological Sciences*, vol. 354, no. 1385, p. 849, 1999.

[5] R. Alexander, *Locomotion of animals*. Blackie Glasgow, 1982.

[6] L. Ting, R. Blickhan, and R. Full, "Dynamic and static stability in hexapedal runners," *Journal of Experimental Biology*, vol. 197, no. 1, p. 251, 1994.

[7] A. Hoover, E. Steltz, and R. Fearing, "RoACH: An autonomous 2.4 g crawling hexapod robot," in *IEEE/RSJ International Conference on Intelligent Robots and Systems*, 2008, pp. 26–33.

[8] P. Birkmeyer, K. Peterson, and R. Fearing, "DASH: A dynamic 16g hexapedal robot," in *IEEE/RSJ International Conference on Intelligent Robots and Systems, 2009. IROS 2009*, 2009, pp. 2683–2689.

[9] U. Saranli, M. Buehler, and D. Koditschek, "RHex: A simple and highly mobile hexapod robot," *The International Journal of Robotics Research*, vol. 20, no. 7, p. 616, 2001.

[10] J. Morrey, B. Lambrecht, A. Horchler, R. Ritzmann, and R. Quinn, "Highly mobile and robust small quadruped robots," in *Proceedings of the IEEE International Conference on Intelligent Robots and Systems*, vol. 1. Citeseer, pp. 82–87.

[11] S. Kim, J. Clark, and M. Cutkosky, "iSprawl: Design and tuning for high-speed autonomous open-loop running," *The International Journal of Robotics Research*, vol. 25, no. 9, p. 903, 2006.

[12] J. Cham, S. Bailey, J. Clark, R. Full, and M. Cutkosky, "Fast and robust: Hexapedal robots via shape deposition manufacturing," *The International Journal of Robotics Research*, vol. 21, no. 10-11, p. 869, 2002.

[13] W. Trimmer, "Microrobots and micromechanical systems," *Sensors and actuators*, vol. 19, no. 3, pp. 267–287, 1989.

[14] A. Baisch and R. Wood, "Design and fabrication of the Harvard ambulatory microrobot," in *14th International Symposium on Robotics Research*, 2009.

[15] M. Spenko, G. Haynes, J. Saunders, M. Cutkosky, A. Rizzi, R. Full, and D. Koditschek, "Biologically inspired climbing with a hexapedal robot," *Journal of Field Robotics*, vol. 25, no. 4, pp. 223–242, 2008.

[16] R. Wood, E. Steltz, and R. Fearing, "Optimal energy density piezoelectric bending actuators," *Sensors & Actuators: A. Physical*, vol. 119, no. 2, pp. 476–488, 2005.

[17] R. Wood, "Design, fabrication, and analysis of a 3DOF, 3cm flapping-wing MAV," in *IEEE/RSJ International Conference on Intelligent Robots and Systems, 2007. IROS 2007*, 2007, pp. 1576–1581.

[18] K. Hoffman and R. Wood, "Towards a multi-segment ambulatory microrobot," in *IEEE International Conference on Robotics and Automation*, 2010.

[19] M. Karpelson, G. Wei, and R. Wood, "Milligram-Scale High-Voltage Power Electronics for Piezoelectric Microrobots," *IEEE International Conference on Robotics and Automation*, vol. 1, 2009.

[20] P. Holmes, D. Koditschek, R. Full, and J. Guckenheimer, "The dynamics of legged locomotion: Models, analyses, and challenges," *Dynamics*, vol. 48, no. 2, pp. 207–304.

[21] J. Seipel, P. Holmes, and R. Full, "Dynamics and stability of insect locomotion: a hexapedal model for horizontal plane motions," *Biological cybernetics*, vol. 91, no. 2, pp. 76–90, 2004.

[22] R. Wood, S. Avadhanula, R. Sahai, E. Steltz, and R. Fearing, "Microrobot design using fiber reinforced composites," *Journal of Mechanical Design*, vol. 130, p. 052304, 2008.

[23] A. Asbeck, S. Kim, M. Cutkosky, W. Provancher, and M. Lanzetta, "Scaling hard vertical surfaces with compliant microspine arrays," *The International Journal of Robotics Research*, vol. 25, no. 12, p. 1165, 2006.

[24] S. Kim, M. Spenko, S. Trujillo, B. Heyneman, D. Santos, and M. Cutkosky, "Smooth vertical surface climbing with directional adhesion," *IEEE Transactions on Robotics*, vol. 24, no. 1, pp. 65–74, 2008.

[25] M. Murphy and M. Sitti, "Waalbot: An agile small-scale wall-climbing robot utilizing dry elastomer adhesives," *IEEE/ASME Transactions on Mechatronics*, vol. 12, no. 3, p. 330, 2007.

[26] M. Karpelson, J. Whitney, G. Wei, and R. Wood, "Energetics of Flapping-Wing Robotic Insects: Towards Autonomous Hovering Flight."